Aperiodic conductivity oscillations in quasiballistic graphene heterojunctions

Milan Begliarbekov,[1] Onejae Sul,[2] Nan Ai,[1] Eui-Hyeok Yang,[2] and Stefan Strauf[1,a)]
[1]*Department of Physics and Engineering Physics, Stevens Institute of Technology, Hoboken, New Jersey 07030, USA*
[2]*Department of Mechanical Engineering, Stevens Institute of Technology, Hoboken, New Jersey 07030, USA*

(Received 5 May 2010; accepted 7 September 2010; published online 23 September 2010)

We observe conductivity oscillations with aperiodic spacing to only one side of the tunneling current in a dual-gated graphene field effect transistor with an n-p-n type potential barrier. The spacing and width of these oscillations were found to be inconsistent with pure Fabry–Perot-type interferences, but are in quantitative agreement with theoretical predictions that attribute them to resonant tunneling through quasibound impurity states. This observation may be understood as another signature of Klein tunneling in graphene heterojunctions and is of importance for future development and modeling of graphene based nanoelectronic devices. © *2010 American Institute of Physics*. [doi:10.1063/1.3493652]

Graphene is a two-dimensional monolayer of carbon atoms that results in a zero-gap semiconductor with outstanding electronic[1] and thermal properties.[2] Unlike in most conventional semiconductors, charge carriers in graphene obey the Dirac equation and are capable of ballistic[3–6] and coherent transport,[7,8] and Veselago lensing.[9] One of the most promising devices for applications in nanoelectronics is the graphene field effect transistor (GFET), which was shown to be capable of ultra high frequency (100 GHz) operation.[10]

Locally gated GFETs give rise to more complex architectures such as n-p-n heterojunctions, which can be realized without physically doping the underlying material. In the conventional transport regime the tunneling current across a potential barrier decreases with increasing barrier energy. In contrast, the chiral Fermions in graphene have been predicted to tunnel through potential barriers with near unitary probability.[6,11] As a result, an increasing tunneling current with increasing barrier energy is expected, analogous to Klein tunneling in quantum electrodynamics. Furthermore, top gated graphene heterojunctions form a Fabry–Perot (FP) type cavity for electron waves, which undergo oscillations in the top gated region due to multiple reflections within the barrier. A π-phase shift in the FP oscillations in a magnetic field was recently observed and understood to be the signature of Klein tunneling in graphene heterojunctions.[5,7,12] Recently, Rossi *et al.* predicted that the residual impurity concentration in partially disordered junctions gives rise to a non-negligible scattering potential V_{sc}, which causes broad and aperiodic conductivity oscillations, which might be understood as another signature of Klein tunneling.[13]

Here we report the experimental observation of aperiodic conductivity oscillations in a quasiballistic GFET. We analyze the spacing and the width of these oscillations, and find that both are better explained by the resonant tunneling model, and cannot be attributed solely to FP oscillations. We further analyze the disorder potential introduced by charged impurities and phonons at elevated temperatures.

A schematic of the dual-gated GFET and the electrical biasing scheme are shown in Fig. 1(a). The graphene flakes were prepared by micromechanical exfoliation of natural graphite onto a p^{++} Si wafer with a thermally grown 300 nm SiO_2 dielectric. The flakes were identified as being single layer from their characteristic Raman spectrum.[14,15] Electron beam lithography was utilized to pattern the graphene flake and to define electrical Cr/Au contacts. A 10 nm Al_2O_3 layer was then evaporated to provide a gate oxide for the subsequent deposition of a 100 nm wide top-gate. An optical micrograph of a device similar to the one used in these experiments is shown in the inset to Fig. 1(c). The top gate was used to apply a local electrostatic potential, thereby creating an n-p-n junction as shown in Fig. 1(b), with a partially graded junction of width D_ω.

The visibility of conductivity oscillations depends strongly on the underlying mobility, coherence length, and the disorder potential. We first characterize the relevant transport parameters in our GFET device by grounding the top gate to the drain electrode. Consequently, carrier transport in the resultant structure is similar to transport in a graphene nanoribbon (GNR). A constant 100 mV source drain bias V_{sd} was applied while the global backgate bias V_{bg}

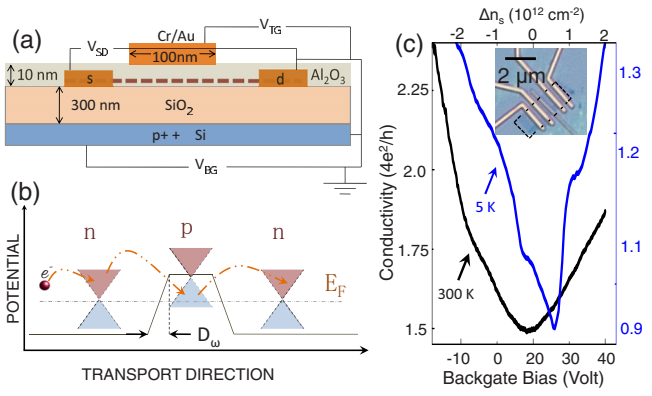

FIG. 1. (Color online) (a) Schematic of device geometry and contacting scheme. (b) Potential profile created by the global backgate and the local top gate as a function of the device length (transport direction) creating an n-p-n junction. (c) RT (300 K) and cryogenic (5 K) conductivities of the device. Inset: optical micrograph of the GFET—the graphene flake has been outlined for clarity.

a)Electronic mail: strauf@stevens.edu.

was varied from −40 to +40 V. The relatively high backgate bias was required since a 300 nm thick dielectric is necessary to provide good optical contrast for the purpose of locating graphene flakes. The mobility can be estimated from the data in Fig. 1(c) using $\mu=(en\rho)^{-1}$, where $n=C_{ox}(V_{bg}-V_{\mathrm{Dirac}})/e$, V_{Dirac} the voltage at the charge neutrality point, and $C_{ox}=115$ aF/μm^2 the oxide capacitance.[3,16,17] At carrier densities of $1-2\times10^{12}$ cm^{-2}, corresponding to back gate voltages of 30–40 V, we estimate a room temperature (RT) mobility of 1120 cm^2 V^{-1} s^{-1} and a cryogenic (5 K) mobility of 3300 cm^2 V^{-1} s^{-1}. The corresponding ballistic mean free paths of $l_e\cong50$ nm at RT and $l_e\cong110$ nm at 5 K were estimated from the scattering time.[16] Note that the $\sigma-V_{bg}$ curve in Fig. 1(c) shows some kinks that most likely originate from tunneling through trapped states which originate from Fermi-level pinning of the local potential at the impurities. These kinks occur on both sides of the global conductivity minimum, and their position changes with each cooldown event.

Furthermore, the two-dimensional sheet carrier density Δn_s was estimated from the geometry of the device and known material properties using $\Delta n_s=\epsilon_o\epsilon_r(V_{bg}-V_{\mathrm{Dirac}})/ed_{ox}$, where $d_{ox}=300$ nm is the oxide thickness, ε_r is the dielectric constant of SiO_2. Similarly, the corresponding top-gate carrier density Δn_{TG} can be calculated from the sheet carrier density Δn_s.[3]

Unlike top and back gate potentials, Δn_s provides unambiguous information about the underlying transport since Δn_s is zero at the charge neutrality point, which is not necessarily located at $V_{bg}=0$. The location of the charge neutrality point away from $V_{bg}=0$ originates from the presence of charged impurities, which contribute to the conductivity σ_{ci} according to:[18,19] $\sigma_{ci}(n)=C_{imp}|\Delta n_s/n_{imp}|$, where $C_{imp}=5\times10^{15}$ V^{-1} s^{-1} is a constant related to the screened Coulomb potential,[20] and n_{imp} is the impurity density. From this equation we find $n_{imp}=6\times10^{11}$ cm^{-2} in our device, the knowledge of which is crucial in identifying the transport regime, and correlating it to the visibility of conductivity oscillations. We further calculate the β parameter, given by $\beta=n'n_i^{-3/2}$, where n' is the slope of the density profile around zero density, and $n_i\equiv e/\mu h$, which differentiates between diffusive and ballistic regimes.[21] Values of $\beta\ll1$ indicate purely diffusive transport, whereas values of $\beta\gg1$ are characteristic of the ballistic regime. In our device $\beta=3.7$ at 5 K, which is indicative of the quasiballistic regime were both ballistic and diffusive transport contributes to the conductivity.

Following the initial characterization of the GNR, the main results have been achieved by applying a bias V_{TG} to the top gate thereby creating the electrostatic potential shown in Fig. 1(b). Using this configuration, we observed an increasing tunneling current with increasing barrier height in the vicinity of the charge neutrality point, as shown in Fig. 2(a). In addition, the onset of up to three conductivity oscillation minima (resistivity maxima) are visible in an aperiodic spacing to only one side of the global conductivity minimum $\Delta n_{tg}=0$.

Similar conductance oscillations have been previously observed,[5,17,22] and analyzed in the context of FP oscillations. The oscillations observed in our device cannot be explained solely by the FP model. In the FP model, where the k-vector is affected by the geometric boundary, the magnitude of the spacing between successive oscillations δ_{ij} can be

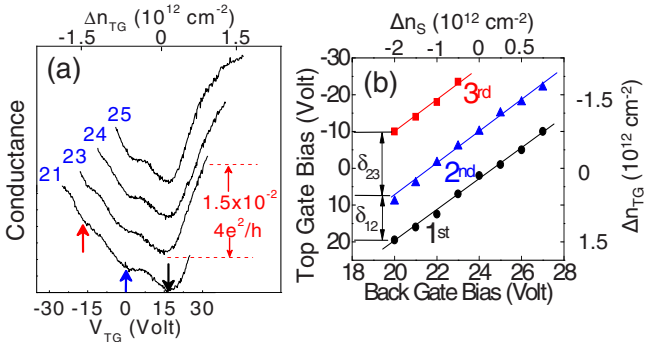

FIG. 2. (Color online) (a) Conductivity as a function of back and top gate bias showing conductivity oscillations characteristic of Klein tunneling. The lines mark conductivity minima. (b) Positions of the peak minima as a function of top and back gate bias. Data recorded at 5 K.

approximated by the condition $k_F(2L)=2\pi$. Consequently the peak spacing becomes $\delta_{ij}=4\sqrt{\pi n_2}/L_c$, where $L_c\cong L_{tg}+2d$, and is thus constant,[22] which would be on the order of 5×10^{10} cm^{-2} in our device. However, in the presence of a scattering potential V_{sc} due to impurity states, the phase shift in the interference θ_{WKB} is given by $\theta_{WKB}=-\int V_{sc}(x',y)dx'$, where the scattering potential V_{sc} is proportional to $V_{sc}\sim\left[V_d(\mathbf{r})+V_{tg}(\mathbf{r})+\frac{1}{2}\int d^2r'(n(\mathbf{r}')/|\mathbf{r}-\mathbf{r}'|)\right]$.[13] Using the above expression for the impurity potential Rossi *et al.* obtain peak spacings of $\delta_{12}=0.85\times10^{12}$ cm^{-2} and $\delta_{23}=1.0\times10^{12}$ cm^{-2} at an impurity concentration $n_{imp}=5\times10^{11}$ cm^{-2}.[13] In our device $\delta_{12}=0.8\times10^{12}$ cm^{-2} and $\delta_{23}=1.1\times10^{12}$ cm^{-2} at the estimated impurity concentration of $n_{imp}=6\times10^{11}$ cm^{-2}.

Furthermore, the observed aperiodic spacing, i.e., $\delta_{12}\neq\delta_{23}$ as shown in Fig. 2(b), can be accounted for by the fact that V_{sc} is a function of topgate bias as well as the carrier concentration inside the junction. This feature cannot be explained solely by the FP model but it is present in the self-consistent simulations using the above expression for the scattering potential. In addition, the width of our oscillations is larger than the theoretically predicted width of FP oscillations,[12] and the experimentally measured width in cleaner devices.[7,5] In contrast, in the presence of V_{sc}, the visibility of these oscillations is strongest at low impurity concentrations and decreases with increasing impurity density, but are predicted to be still visible at our experimental values of $n_{imp}=6\times10^{11}$ cm^{-2}, while both the theoretical and experimental width are estimated to be about 0.4×10^{12} cm^{-2}, and thus comparable. Consequently, the magnitude of oscillation spacing and width in our device is best explained by resonant tunneling through quasibound impurities.

Finally, we analyze the temperature dependence of the conductivity oscillations to study the influence of the degradation of the ballistic mean free path and polar optical phonons on the observed oscillations. The magnitude of oscillations diminishes at higher temperatures as shown in Fig. 3(a). Figure 3(b) shows a log-log plot of the amplitude of the first resistance oscillation peak ΔI as a function of temperature, which vanishes at about 85 K. To understand what happens at this particular temperature we recorded the temperature dependence of the GFET resistivity with the top-gate grounded as shown in Fig. 3(c). The observed exponential increase in resistivity is consistent with previous investigations.[18,23] The fitted solid curves in Fig. 3(c) correspond to the phonon contribution to the resistivity ρ_{ph} as

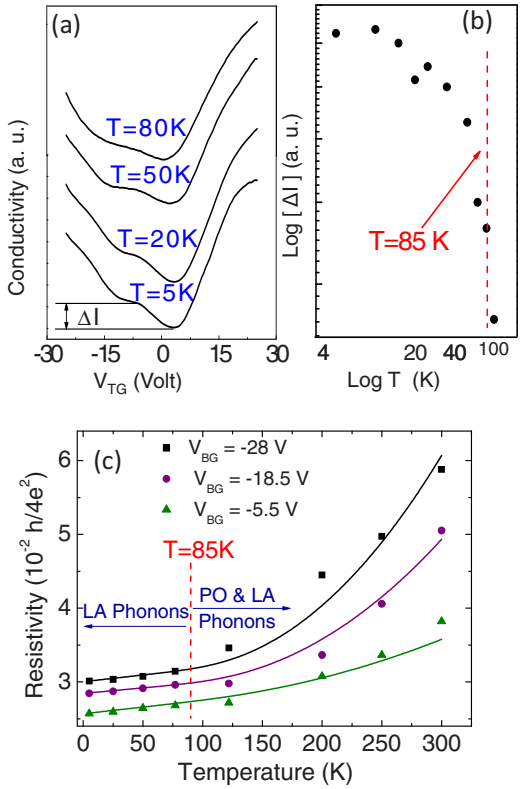

FIG. 3. (Color online) (a) Temperature dependence of the conductivity oscillations. (b) Amplitude ΔI of the first oscillation with respect to the minimum between the first and second peak. (c) Temperature dependence of the resistivity as a function of several back-gate biases.

given by $\rho_{ph}=\rho_0(V_{BG})+\rho_{LA}(T)+\rho_{PO}(V_{BG},T)$, where $\rho_0(V_{BG})$ is the residual resistivity, and ρ_{LA} and ρ_{PO} are due to acoustic and polar optical phonons, respectively.[18] The only free parameter in ρ_{LA} is the acoustic deformation potential D_A, which we extract from the linear part in Fig. 3(c) to be $D_A=15\pm3$ eV. The contribution to the total phonon resistivity due to ρ_{PO} was analyzed following Ref. 24, and is in good agreement with our data [see fit in Fig. 3(c)].

Thus, the underlying scattering mechanism most likely originates from polar phonon injection from the underlying SiO_2, which set in above 85 K. These phonons cause carrier scattering and thereby degrade the ballistic mean free path. As a consequence, transport through the barrier becomes purely diffusive, since $l_e\cong110$ nm at 5 K degraded to values smaller than the top gate length of 100 nm which defines the n-p-n junction. Therefore, the conductance oscillations vanish at about 85 K when the GFET transitions from quasiballistic to diffusive transport through the barrier due to the onset of polar optical phonons.

In summary, we fabricated an GFET with an n-p-n type potential barrier and observed aperiodic conductivity oscillations in the quasiballistic regime ($\beta=3.7$). The peak spacing cannot be explained solely by the FP model, but is correctly predicted when resonant tunneling through impurity states is taken into account, in agreement with recent theoretical predictions. The observation of resonant tunneling through impurity states may be understood as another signature of Klein tunneling in graphene heterojunctions and is of importance for future development of high performance GFETs.

We thank Kitu Kumar, Steve Tsai, and Anderson Tsai for assistance with sample preparation. Partial financial support was provided by the NSF GK-12 under Grant No. DGE-0742462 and by AFOSR, Award No. FA9550-08-1-013. We thank the Center for Functional Nanomaterials of the Brookhaven National Laboratory, Contract No. DE-AC02-98CH10886, for the use of their clean rooms.

[1]A. K. Geim and K. S. Novoselov, Nature Mater. **6**, 183 (2007).
[2]A. A. Balandin, S. Ghosh, W. Bao, I. Calizo, D. Teweldebrhan, F. Miao, and C. N. Lau, Nano Lett. **8**, 902 (2008).
[3]N. Stander, B. Huard, and D. Goldhaber-Gordon, Phys. Rev. Lett. **102**, 026807 (2009).
[4]J. R. Williams, L. DiCarlo, and C. M. Marcus, Science **317**, 638 (2007).
[5]R. V. Gorbachev, A. S. Mayorov, A. K. Savchenko, D. W. Horsell, and F. Guinea, Nano Lett. **8**, 1995 (2008).
[6]C. W. J. Beenakker, Rev. Mod. Phys. **80**, 1337 (2008).
[7]A. F. Young and P. Kim, Nat. Phys. **5**, 222 (2009).
[8]S. Russo, J. B. Oostinga, D. Wehenkel, H. B. Heersche, S. S. Sobhani, L. M. K. Vandersypen, and A. F. Morpurgo, Phys. Rev. B **77**, 085413 (2008).
[9]V. V. Cheianov, V. Fal'ko, and B. L. Altshuler, Science **315**, 1252 (2007).
[10]Y.-M. Lin, C. Dimitrakopoulos, K. A. Jenkins, D. B. Farmer, H.-Y. Chiu, A. Grill, and Ph. Avouris, Science **327**, 662 (2010).
[11]M. I. Katsnelson, K. S. Novoselov, and A. K. Geim, Nat. Phys. **2**, 620 (2006).
[12]V. Shytov, M. S. Rudner, and L. S. Levitov, Phys. Rev. Lett. **101**, 156804 (2008).
[13]E. Rossi, J. H. Bardarson, P. W. Brouwer, and S. D. Sarma, Phys. Rev. B **81**, 121408(R) (2010).
[14]M. Begliarbekov, O. Sul, S. Kalliakos, E.-H. Yang, and S. Strauf, Appl. Phys. Lett. **97**, 031908 (2010).
[15]A. C. Ferrari, J. C. Meyer, V. Scardaci, C. Casiraghi, M. Lazzeri, F. Mauri, S. Piscanec, D. Jiang, K. S. Novoselov, S. Roth, and A. K. Geim, Phys. Rev. Lett. **97**, 187401 (2006).
[16]Y.-W. Tan, Y. Zhang, K. Bolotin, Y. Zhao, S. Adam, E. H. Hwang, S. Das Sarma, H. L. Stormer, and P. Kim, Phys. Rev. Lett. **99**, 246803 (2007).
[17]B. Huard, J. A. Sulpizio, N. Stander, K. Todd, B. Yang, and D. Goldhaber-Gordon, Phys. Rev. Lett. **98**, 236803 (2007).
[18]J.-H. Chen, C. Jang, M. Ishigami, S. Xiao, E. D. Williams, and M. S. Fuhrer, Solid State Commun. **149**, 1080 (2009).
[19]K. Nomura and A. H. MacDonald, Phys. Rev. Lett. **98**, 076602 (2007).
[20]E. H. Hwang, S. Adam, and S. D. Sarma, Phys. Rev. Lett. **98**, 186806 (2007).
[21]M. M. Fogler, D. S. Novikov, L. I. Glazman, and B. I. Shklovshii, Phys. Rev. B **77**, 075420 (2008).
[22]J. Velasco, G. Liu, W. Bao, and C. N. Lau, New J. Phys. **11**, 095008 (2009).
[23]I. Meric, M. Y. Han, A. F. Young, B. Ozyilmaz, P. Kim, and K. L. Shepard, Nat. Nanotechnol. **3**, 654 (2008).
[24]S. Fratini and F. Guinea, Phys. Rev. B **77**, 195415 (2008).